JOURNAL OF THE PHYSICAL SOCIETY OF JAPAN, Vol. 43, No. 5, NOVEMBER, 1977

Screening Effect and Quantum Transport in a Silicon Inversion Layer in Strong Magnetic Fields*

Tsuneya ANDO

Department of Physics, University of Tokyo, 7-3-1, Hongo, Bunkyo-ku, Tokyo 113

(Received June 13, 1977)

The broadening of Landau levels and the transport quantities, such as the transverse and Hall conductivity and cyclotron resonance linewidth, are calculated in an inversion layer on the (100) surface of *p*-type Si at zero temperature. Main scattering mechanisms are assumed to be charged impurity scattering and surface roughness scattering. A new expression for the surface roughness scattering is obtained. The self-consistent Born approximation is employed for the effect of scattering, and the random phase approximation for the screening. Because of the singular density of states the screening depends on the position of the Fermi level and becomes weak when it lies at the tail region of each Landau level. Scattering potentials become strong and of slowly varying type in this case. Except such a special case, overall features agree with the results obtained for short-ranged scatterers.

§1. Introduction

In accumulation and inversion layers on semiconductor surfaces the motion of electrons in the direction normal to the surface or interface is quantized, and the electronic states form two-dimensional energy bands called electric subbands. Under the usual conditions at low temperatures only the ground (lowest) subband is occupied by electrons, and the system can be considered quasi-two-dimensional. In addition to the two-dimensionality this system is characterized by the fact that the number density of electrons N_s can be changed over a wide range by varying the strength of the electric field applied perpendicular to the surface. Consequently there is considerable current interest in its electronic properties such as transport phenomena and effects of electron-electron interactions.

Especially there have been numerous experimental and theoretical investigations on scattering mechanisms and electron transport in zero or a weak magnetic field.[1-4] In the course of such study two mechanisms have been known to contribute to the scattering of electrons in inversion layers of Si at low temperatures—charged impurity scattering and surface roughness scattering. The former is believed to arise from charges in the oxide near the Si–SiO_2 interface rather than impurity ions in Si, and has theoretically been studied first by Stern and Howard,[2] and later by many others.[1-3] The latter is believed to arise from surface asperities whose exact nature is not known yet, and has theoretically been studied first by Prange and Nee in case of magnetic surface states in metals.[5] Many authors have applied this theory to the inversion layers, but it is not complete in our system as will be shown in the following. In any case consideration of these two mechanisms explains the characteristic feature of the mobility common to all the samples at low temperatures. The mobility increases first, takes a maximum value of typically $\mu \sim 10^4$ cm^2/Vs at N_s of $0.3 \sim 0.7 \times 10^{12}$ cm^{-2}, and then decreases with increasing N_s. Further screening of scattering potentials by free electrons in the inversion layers has been shown to play an important role in determining the mobility.

When a strong magnetic field is applied normal to the surface, the energy spectrum of the two-dimensional system becomes discrete because of the complete quantization of the orbital motion. This system provides an ideal tool for the study of the quantum

* A preliminary report of a part of this work was presented at 3-rd Int. Conf. Application of High Magnetic Fields in Semiconductor Phys., Würzburg, 1976.

transport phenomena. As a matter of fact, there has been a number of theoretical and experimental work on phenomena such as galvanomagnetic effects[6–16] and cyclotron resonance.[17–19] So far as the gross features of these phenomena are concerned, the excellent agreement between theory and experiments has been obtained when phenomenologically introduced short-ranged scatterers are assumed. In detail, however, there still remain some experimental results which can not be explained by such simple short-ranged scatterers.

In this paper we apply a previous theory of the quantum transport in the two-dimensional system[9,10] to actual inversion layers on the (100) surface of p-type Si. We assume the two mechanisms discussed above, and calculate various transport quantities like the width of each Landau level, the transverse conductivity σ_{xx}, the Hall conductivity σ_{xy}, and the width of the cyclotron resonance. As for the effect of the scattering we employ the self-consistent Born approximation (SCBA), which is the simplest one free from the difficulty of divergence caused by the discrete density of states and has worked well in explaining characteristics of the transport phenomena of this system. As might be expected the screening effect again plays an important role in determining these quantities. As a result of the singular density of states the screening depends strongly on the broadening and on the position of the Fermi level at low temperatures. Thus we have to calculate the broadening and the screening in a self-consistent manner. The screening is included by using a dielectric function calculated in the random phase approximation (RPA).[20]

In §2 the two scattering mechanisms are introduced. A complete form of the effective potential for surface roughness is obtained and evaluated in terms of the Stern-Howard variational wave function. The roughness-limited mobility is explicitly calculated and compared with experiments in the absence of a magnetic field. The results qualitatively explains characteristic features of the experiments. Explicit expressions of various transport quantities in strong magnetic fields are given in §3. Several examples of the results of numerical calculation are presented in §4. The screening depends strongly on the position of the Fermi level and becomes small when the Fermi level lies at the tail region of each Landau level. Consequently the scattering potentials become strong and of slowly-varying type and the level width becomes very large. The cyclotron resonance linewidth does not show such a singular behavior. Except this case, however, the width in strong magnetic fields is shown to be related to the mobility in the absence of a magnetic field as has been suggested previously, and overall features are in good agreement with those for short-ranged scatterers. The screening effect becomes slightly weaker and the peak value of the transverse conductivity decreases with decreasing magnetic field, which qualitatively explains the recent experiments of Lakhani and Stiles.[13] To get quantitative agreement, however, we must assume additional scattering mechanisms corresponding to short-ranged scatterers especially at relatively low N_s.

§2. Scattering Mechanisms

2.1 *Preliminaries*

We consider the system described by the following Hamiltonian.

$$\mathcal{H}=\mathcal{H}_0+\mathcal{H}', \tag{2.1}$$

with

$$\mathcal{H}_0=\frac{1}{2m_t}\left(\boldsymbol{p}+\frac{e}{c}\boldsymbol{A}\right)^2+\frac{1}{2m_l}p_z^2+V(z), \tag{2.2}$$

and

$$V(z)=V_0\theta(-z)+v_{\mathrm{depl}}(z)+v_s(z)+v_{\mathrm{image}}(z), \tag{2.3}$$

where z is the distance into the bulk measured from the surface (xy plane), $\boldsymbol{r}$ and $\boldsymbol{p}$ are two-dimensional vectors in the xy plane, and $\theta(z)$ is the step function. The first term of the right hand side of eq. (2.3) describes the potential barrier at Si–SiO_2 interface and V_0 is assumed to be sufficiently large. The second corresponds to the potential of the charges in the depletion layer and is replaced by a uniform electric field.

$$v_{\mathrm{depl}}(z)=\frac{4\pi e^2}{\kappa_s}N_{\mathrm{depl}}z, \tag{2.4}$$

where κ_s is the static dielectric constant of Si and N_{depl} is the concentration of the fixed

charges in the depletion layer. This replacement is justified since the thickness of the inversion layer ($\lesssim 10^2$ A) is much smaller than that of the depletion layer ($\sim 10^4$ A, typically). The third term is the Hartree potential of electrons themselves and has been obtained by solving Poisson's equation.

$$v_s(z)=\frac{4\pi e^2}{\kappa_s}N_s\left[z-\int_0^z \mathrm{d}z'(z-z')n(z')\right], \quad (2.5)$$

where $n(z)$ is the density distribution normalized to unity. The last term represents the repulsive image potential, given by

$$v_{\mathrm{image}}(z)=\frac{(\kappa_s-\kappa_{ox})e^2}{4\kappa_s(\kappa_s+\kappa_{ox})z}, \quad (2.6)$$

where κ_{ox} is the static dielectric constant of the oxide. The last term $\mathscr{H}'$ of eq. (2.1) describes additional scattering potentials arising from the scatterers and will be evaluated in the later part of this section.

The energy spectra for the two-dimensional motion in the xy plane are given by discrete Landau levels, whose energy is given by $E_N=(N+1/2)\hbar\omega_c$ with $\omega_c=eH/m_tc$. The wave function $\zeta_n(z)$ of the n-th subband satisfies

$$\left[-\frac{\hbar^2}{2m_t}\frac{\mathrm{d}^2}{\mathrm{d}z^2}+V(z)\right]\zeta_n(z)=\varepsilon_n\zeta_n(z), \quad (2.7)$$

where ε_n is the bottom of the subband. Throughout this paper we assume that only the ground subband denoted by 0 is occupied by electrons, *i.e.* $n(z)=\zeta_0(z)^2$. Further in the actual calculation we use the Stern-Howard variational wave function,[2] given by

$$\zeta_{\mathrm{SH}}(z)=\left(\frac{b^3}{2}\right)^{1/2}z\exp\left(-\frac{b}{2}z\right), \quad (2.8)$$

instead of the exact wave function $\zeta_0(z)$. By the standard variational procedure we have $b=b_{\mathrm{SH}}/\beta$, with

$$b_{\mathrm{SH}}^3=\frac{48\pi e^2m_t}{\kappa_s\hbar^2}\left(N_{\mathrm{depl}}+\frac{11}{32}N_s\right), \quad (2.9)$$

$$\beta=\delta^{1/2}\cosh\left(\frac{1}{3}\cosh^{-1}4\delta^{-3/2}\right) \quad (2.10)$$

and

$$\delta=\frac{3}{8}\frac{m_t(\kappa_s-\kappa_{ox})e^2}{\hbar^2b_{\mathrm{SH}}(\kappa_s+\kappa_{ox})\kappa_s}. \quad (2.11)$$

2.2 *Charged impurities in SiO_2*

Since many authors have investigated the effects of charged impurities, we shall briefly write down equations necessary for the following discussion. The potential of a charged impurity located at $(\boldsymbol{R}, Z)$ $(Z<0)$ is given by

$$V(\boldsymbol{r}-\boldsymbol{R}, z-Z)=\sum_{\boldsymbol{q}}\frac{2\pi e^2}{\bar{\kappa}q}\exp\left[-q(z-Z)+i\boldsymbol{q}\cdot(\boldsymbol{r}-\boldsymbol{R})\right], \quad (2.12)$$

where $\bar{\kappa}=(\kappa_s+\kappa_{ox})/2$. The effective two-dimensional potential for the ground subband becomes

$$v(\boldsymbol{r}-\boldsymbol{R};Z)=\sum_{\boldsymbol{q}}\frac{2\pi e^2}{\bar{\kappa}q}\left(1+\frac{q}{b}\right)^{-3}\exp\left[qZ+i\boldsymbol{q}\cdot(\boldsymbol{r}-\boldsymbol{R})\right], \quad (2.13)$$

where we have used the variational wave function. The screening effect can be taken into account if we replace the above by

$$v(\boldsymbol{r}-\boldsymbol{R};Z)=\sum_{\boldsymbol{q}}\frac{2\pi e^2}{\bar{\kappa}q\varepsilon(q)}\left(1+\frac{q}{b}\right)^{-3}\exp\left[qZ+i\boldsymbol{q}\cdot(\boldsymbol{r}-\boldsymbol{R})\right], \quad (2.14)$$

where $\varepsilon(q)$ is the dielectric function, given in the RPA by

$$\varepsilon(q)=1+\frac{2\pi e^2}{\bar{\kappa}q}F(q)\Pi(q). \quad (2.15)^{20}$$

Here $F(q)$ is the form factor, given by

$$F(q)=\frac{1}{2}\left\{\left(1+\frac{\kappa_{ox}}{\kappa_s}\right)\left[1+\frac{9}{8}\frac{q}{b}+\frac{3}{8}\left(\frac{q}{b}\right)^2\right]\left(1+\frac{q}{b}\right)^{-3}+\left(1-\frac{\kappa_{ox}}{\kappa_s}\right)\left(1+\frac{q}{b}\right)^{-6}\right\}. \quad (2.16)$$

In the absence of a magnetic field the polarization part $\Pi(q)$ becomes

$$\Pi(q)=2g_v\frac{m_t}{2\pi\hbar^2}\left\{1-\theta(q-2k_F)\left[1-\left(\frac{2k_F}{q}\right)^2\right]^{1/2}\right\}, \quad (2.17)^{21}$$

where k_F is the Fermi wave vector and $g_v=2$ is the valley degeneracy.

As has been done by Matsumoto and Uemura[3] we assume in this paper that charged impurities are distributed randomly in the oxide. The relaxation time limited by those is given by

$$\frac{1}{\tau_i}=\frac{2\pi}{\hbar}\frac{1}{2}N_i\frac{m_t}{2\pi\hbar^2}\int_0^{2\pi}\frac{d\theta}{2\pi}\left[\frac{2\pi e^2}{2\bar{\kappa}k_F\sin\frac{\theta}{2}\,\varepsilon(2k_F\sin\frac{\theta}{2})}\right]^2\left(1+\frac{2k_F\sin\frac{\theta}{2}}{b}\right)^{-6}\frac{1-\cos\theta}{2k_F\sin\frac{\theta}{2}}, \tag{2.18}$$

where N_i is the concentration of impurities in a unit volume.

2.3 *Surface roughness scattering*

Let $\Delta(\boldsymbol{r})$ be the deviation of the interface from the flat xy plane. The change of the barrier potential is given by

$$V_{SR}^{(1)}(\boldsymbol{r}, z)=V_0\theta(-z+\Delta(\boldsymbol{r}))-V_0\theta(-z). \tag{2.19}$$

For sufficiently large V_0 the matrix element between the n-th and n'-th subband is easily shown to be

$$\int dz\,\zeta_n^*(z)V_{SR}^{(1)}(\boldsymbol{r}, z)\zeta_{n'}(z)=\frac{\hbar^2}{2m_l}\Delta(\boldsymbol{r})\frac{d\zeta_n^*}{dz}\frac{d\zeta_{n'}}{dz}\bigg|_{z=0}, \tag{2.20}$$

which is the expression obtained first by Prange and Nee[5] for the magnetic surface states.* Further for the diagonal element we can show that

$$\int dz\,\zeta_n^*(z)V_{SR}^{(1)}(\boldsymbol{r}, z)\zeta_n(z)=\Delta(\boldsymbol{r})\int dz|\zeta_n(z)|^2\left(\frac{\partial v_{\text{depl}}}{\partial z}+\frac{\partial v_s}{\partial z}+\frac{\partial v_{\text{image}}}{\partial z}\right). \tag{2.21}$$

This can be proved by using the identity:

$$\int dz\,\zeta_n^*(z)\frac{\partial V}{\partial z}\zeta_n(z)=0, \tag{2.22}$$

which simply means that the average force electrons feel vanishes for a bound state. Equation (2.21) was first obtained by Matsumoto and Uemura,[3] although they neglected the image potential. When only the ground subband is occupied by electrons, one can show that

$$\int dz|\zeta_0(z)|^2\left(\frac{\partial v_{\text{depl}}}{\partial z}+\frac{\partial v_s}{\partial z}\right)=\frac{4\pi e^2}{\kappa_s}\left(N_{\text{depl}}+\frac{1}{2}N_s\right). \tag{2.23}$$[22]

Equations (2.20) and (2.21) are completely equivalent, if we use the exact wave function. In case of variational wave functions, however, we should rather use eq. (2.21), since it gives the exact result (2.23) while eq. (2.20) does not.

All the previous theories of the surface roughness scattering in inversion layers considered only the above mentioned change of the barrier potential caused by $\Delta(\boldsymbol{r})$. Actually, however, the electric field distribution is modified by $\Delta(\boldsymbol{r})$ near the interface, and this effect is comparable to the above effect. This change of the field distribution is evaluated in the Appendix. The result is given as follows:

$$\begin{aligned}V_{SR}^{(2)}(\boldsymbol{r}, z)=&-\Delta(\boldsymbol{r})\frac{\partial}{\partial z}(v_{\text{depl}}+v_s+v_{\text{image}})+\frac{4\pi e^2}{\bar{\kappa}}\left(N_{\text{depl}}+\frac{1}{2}N_s\right)\Delta(\boldsymbol{r})\\&-\sum_{\boldsymbol{q}}\frac{2\pi e^2}{\kappa_s q}N_s\Delta(\boldsymbol{q})\,e^{i\boldsymbol{q}\cdot\boldsymbol{r}}\int[e^{-q|z-z'|}+q|z-z'|]\frac{\partial n(z')}{\partial z'}dz'\\&-\sum_{\boldsymbol{q}}\frac{2\pi e^2(\kappa_s-\kappa_{ox})}{\kappa_s(\kappa_s+\kappa_{ox})q}N_s\Delta(\boldsymbol{q})\,e^{i\boldsymbol{q}\cdot\boldsymbol{r}}\int[e^{-q(z+z')}+qz']\frac{\partial n(z')}{\partial z'}dz'\end{aligned}$$

* In our model we have assumed that the motion of electrons is described by the same effective masses in the whole space. Even if one assumes different masses for $z<0$, one gets the present result for sufficiently large V_0.

$$+\sum_{\boldsymbol{q}}\frac{4\pi e^2(\kappa_s-\kappa_{ox})}{\kappa_s(\kappa_s+\kappa_{ox})}(N_s+N_{\mathrm{depl}})\Delta(\boldsymbol{q})\,\mathrm{e}^{i\boldsymbol{q}\cdot\boldsymbol{r}}(\mathrm{e}^{-qz}-1)$$
$$+\sum_{\boldsymbol{q}}\frac{(\kappa_s-\kappa_{ox})e^2}{4\kappa_s(\kappa_s+\kappa_{ox})}q^2\Delta(\boldsymbol{q})\,\mathrm{e}^{i\boldsymbol{q}\cdot\boldsymbol{r}}\left[\frac{K_1(qz)}{qz}-\frac{1}{(qz)^2}-\frac{1}{2}\frac{\kappa_s-\kappa_{ox}}{\kappa_s+\kappa_{ox}}K_0(qz)\right], \tag{2.24}$$

where K_0 and K_1 are the modified Bessel function and

$$\Delta(\boldsymbol{r})=\sum_{\boldsymbol{q}}\Delta(\boldsymbol{q})\,\mathrm{e}^{i\boldsymbol{q}\cdot\boldsymbol{r}}. \tag{2.25}$$

The effective surface roughness potential is obtained by $V_{SR}=V_{SR}^{(1)}+V_{SR}^{(2)}$.

After a little manipulation the effective surface roughness potential for the ground subband becomes

$$v_{SR}(\boldsymbol{r})=\int\mathrm{d}z\,\zeta_0^*(z)V_{SR}\zeta_0(z)=\sum_{\boldsymbol{q}}\Delta(\boldsymbol{q})\Gamma(\boldsymbol{q})\,\mathrm{e}^{i\boldsymbol{q}\cdot\boldsymbol{r}}, \tag{2.26}$$

with

$$\Gamma(\boldsymbol{q})=\gamma(\boldsymbol{q})+\gamma_{\mathrm{image}}(\boldsymbol{q}), \tag{2.27}$$

where

$$\gamma(q)=\frac{4\pi e^2}{\bar{\kappa}}\left(N_{\mathrm{depl}}+\frac{1}{2}N_s\right)-\frac{4\pi e^2(\kappa_s-\kappa_{ox})}{\kappa_s(\kappa_s+\kappa_{ox})}(N_{\mathrm{depl}}+N_s)\left[1-\left(1+\frac{q}{b}\right)^{-3}\right]$$
$$+\frac{2\pi e^2(\kappa_s-\kappa_{ox})}{\kappa_s(\kappa_s+\kappa_{ox})}N_s\left[1-\left(1+\frac{q}{b}\right)^{-6}\right], \tag{2.28}$$

and

$$\gamma_{\mathrm{image}}(q)=-\frac{(\kappa_s-\kappa_{ox})e^2}{4\kappa_s(\kappa_s+\kappa_{ox})}\frac{1}{2}q^2\left\{\left[1-\left(\frac{q}{b}\right)^2\right]^{-1}\left[\left[1-\left(\frac{q}{b}\right)^2\right]^{-1/2}\ln\frac{(1+q/b)^{1/2}+(1-q/b)^{1/2}}{(1+q/b)^{1/2}-(1-q/b)^{1/2}}-1\right]\right.$$
$$\left.+\frac{3}{2}\frac{\kappa_s-\kappa_{ox}}{\kappa_s+\kappa_{ox}}\left[1-\left(\frac{q}{b}\right)^2\right]^{-2}\left[\left[1-\left(\frac{q}{b}\right)^2\right]^{-1/2}\left[\frac{2}{3}+\frac{1}{3}\left(\frac{q}{b}\right)^2\right]\ln\frac{(1+q/b)^{1/2}+(1-q/b)^{1/2}}{(1+q/b)^{1/2}-(1-q/b)^{1/2}}-1\right]\right\}, \tag{2.29a}$$

for $q/b<1$ and

$$\gamma_{\mathrm{image}}(q)=-\frac{(\kappa_s-\kappa_{ox})e^2}{4\kappa_s(\kappa_s+\kappa_{ox})}\frac{1}{2}q^2\left\{\left[\left(\frac{q}{b}\right)^2-1\right]^{-1}\left[1-2\left[\left(\frac{q}{b}\right)^2-1\right]^{-1/2}\tan^{-1}\frac{q/b-1}{q/b+1}\right]\right.$$
$$\left.+\frac{3}{2}\frac{\kappa_s-\kappa_{ox}}{\kappa_s+\kappa_{ox}}\left[\left(\frac{q}{b}\right)^2-1\right]^{-2}\left[\left[\left(\frac{q}{b}\right)^2-1\right]^{-1/2}\left[\frac{2}{3}+\frac{1}{3}\left(\frac{q}{b}\right)^2\right]2\tan^{-1}\frac{q/b-1}{q/b+1}-1\right]\right\}, \tag{2.29b}$$

for $q/b>1$. We have used the variational wave function. For $q/b\ll1$ we have

$$\gamma(q)=\frac{4\pi e^2}{\bar{\kappa}}\left(N_{\mathrm{depl}}+\frac{1}{2}N_s\right), \tag{2.30}$$

and for $q/b\gg1$

$$\gamma(q)=\frac{4\pi e^2}{\kappa_s}\left(N_{\mathrm{depl}}+\frac{1}{2}N_s\right). \tag{2.31}$$

Thus the matrix element $\gamma(q)$ decreases with increasing q and approaches to the value obtained by Matsumoto and Uemura.[3)]

Let us assume as usual the roughness with the mean square height Δ and the lateral spatial decay rate d, i.e.

$$\langle\Delta(\boldsymbol{r})\Delta(\boldsymbol{r}')\rangle=\Delta^2\exp\left[-\frac{(\boldsymbol{r}-\boldsymbol{r}')^2}{d^2}\right], \tag{2.32}$$

where $\langle \ldots \rangle$ means the sample average.[3] In this model the relaxation time becomes

$$\frac{1}{\tau_{SR}}=\frac{2\pi}{\hbar}\frac{m_t}{\hbar^2}(\Delta d)^2\int_0^{2\pi}\frac{d\theta}{2\pi}\sin^2\frac{\theta}{2}\exp\left(-k_F^2d^2\sin^2\frac{\theta}{2}\right)\Gamma\left(2k_F\sin\frac{\theta}{2}\right)^2\varepsilon\left(2k_F\sin\frac{\theta}{2}\right)^{-2}. \quad (2.33)$$

This relaxation time is calculated numerically, and some examples of the results are given in Fig. 1 together with the experiments of Hartstein *et al.*[4] The inverse of the mobility $\mu_{SR}=e\tau_{SR}/m_t$ is plotted as a function of $(N_s+N_{depl})^2$. They have experimentally subtracted the contribution of ionized impurity scattering from their results and have shown that the resulting mobility attributed to the surface roughness scattering is a function of $(N_s+N_{depl})^2$. The calculated mobility is roughly a function of $(N_s+N_{depl})^2$ below $N_s\sim 7\times 10^{12}$ cm^{-2} for reasonable values of N_{depl}. At higher N_s the result deviates from the relation. Actually, however, higher subbands become occupied by electrons at those concentrations,[23,24] and we must calculate the conductivity or the mobility in such cases. This problem is out of the scope of the present paper and is left for future study.

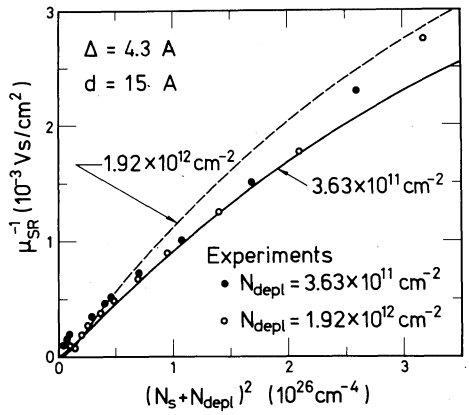

Fig. 1. Calculated mobility limited by surface roughness and examples of experimental results for two different values of depletion charges: $N_{depl}=3.63\times10^{11}$ cm^{-2} and 1.92×10^{12} cm^{-2}. We have assumed that $\Delta=4.3$ A and $d=15$ A.

§3. Screening Effect and Quantum Transport

3.1 *Broadening of Landau levels*

In sufficiently strong magnetic fields the SCBA gives the density of states for the N-th Landau level

$$D(E)=\frac{1}{2\pi l^2}\frac{2}{\pi\Gamma_N}\left[1-\left(\frac{E-E_N}{\Gamma_N}\right)^2\right]^{1/2}, \quad (3.1)^9$$

with $l^2=c\hbar/eH$. The width Γ_N is given by eq. (2.13) of ref. 17. In taking into account the screening effect the momentum representation is convenient. In our model described in the previous section we have

$$\Gamma_N^2=4N_i\sum_q\frac{1}{2q}\left[\frac{2\pi e^2}{\bar{\kappa}q\varepsilon(q)}\right]^2\left(1+\frac{q}{b}\right)^{-6}J_{NN}(lq)^2+4\cdot2\pi(\Delta d)^2\sum_q\left[\frac{\Gamma(q)}{\varepsilon(q)}\right]^2\exp\left(-\frac{1}{4}q^2d^2\right)J_{NN}(lq)^2, \quad (3.2)$$

with

$$J_{NN'}(x)=\sqrt{\frac{N'!}{N!}}\left(\frac{x}{\sqrt{2}}\right)^{N-N'}L_{N'}^{N-N'}\left(\frac{x^2}{2}\right)\exp\left(-\frac{x^2}{4}\right), \quad (3.3)$$

where $L_n^m(x)$ is the associated Laguerre polynomial.

In eq. (3.2) we should use the dielectric function in strong magnetic fields, which is given by the same expression as eq. (2.15) except $\Pi(q)$. The polarization part $\Pi(q)$ in strong magnetic field has been calculated in ref. 20 for short-ranged scatterers, where the width Γ_N is independent of N. Instead of calculating $\Pi(q)$ for our model scatterers we shall use this result, replacing Γ by Γ_N in eqs. (2.36) and (2.37) of ref. 20, when the Fermi level E_F lies in the N-th Landau level. This approximation is sufficient for the present purpose, since the screening is expected not to depend on the range strongly and the resulting potential is relatively of short range except when E_F lies at the tails of the density of states. As one can easily see, the dielectric function is a function of the width Γ_N, i.e. proportional to Γ_N^{-1} roughly speaking. The width itself is dependent on the screening as is evident from eq. (3.2). Thus we have to determine the width and the screening self-consistently.

3.2 The transverse conductivity

When E_F lies in the N-th Landau level, the transverse conductivity is given by

$$\sigma_{xx}=\int dE\left(-\frac{\partial f}{\partial E}\right)\frac{e^2}{\pi^2\hbar}\left(\frac{\Gamma_N^{xx}}{\Gamma_N}\right)^2\left[1-\left(\frac{E-E_N}{\Gamma_N}\right)^2\right], \tag{3.3}^{9)}$$

where f is the Fermi distribution function. In case of short-ranged scatterers we have $(\Gamma_N^{xx})^2=(N+1/2)\Gamma^2$ and the peak value depends only on the Landau level index N and not on H and strength of scattering.[7] In our model we have

$$(\Gamma_N^{xx})^2=N_i\sum_q\frac{1}{2q}(ql)^2\left[\frac{2\pi e^2}{\bar{\kappa}q\varepsilon(q)}\right]^2\left(1+\frac{q}{b}\right)^{-6}J_{NN}(lq)^2$$
$$+2\pi(\Delta d)^2\sum_q(ql)^2\left[\frac{\Gamma(q)}{\varepsilon(q)}\right]^2\exp\left(-\frac{1}{4}q^2d^2\right)J_{NN}(lq)^2. \tag{3.4}$$

3.3 The Hall conductivity

The Hall conductivity can be written as

$$\sigma_{xy}=-\frac{nec}{H}+\Delta\sigma_{xy}, \tag{3.5}$$

where $\Delta\sigma_{xy}$ represents the effect of scattering and is given by

$$\Delta\sigma_{xy}=\int dE\left(-\frac{\partial f}{\partial E}\right)\frac{e^2}{\pi^2\hbar}\frac{(\Gamma_N^{xy})^4}{\hbar\omega_c(\Gamma_N)^3}\left[1-\left(\frac{E-E_N}{\Gamma_N}\right)^2\right]^{3/2}. \tag{3.6}^{11)}$$

In case of short-ranged scatterers we have $(\Gamma_N^{xy})^4=(N+1/2)\Gamma^4$, and the peak value of $\Delta\sigma_{xy}$ is given by $(e^2/\pi^2\hbar)(N+1/2)\Gamma/\hbar\omega_c$. In our model we have

$$(\Gamma_N^{xy})^4=\sum_{\pm}(\Gamma_N^{\pm})^4, \tag{3.7}$$

with

$$(\Gamma_N^{\pm})^2=\pm 2N_i\sum_q\frac{1}{2q}ql\left[\frac{2\pi e^2}{\bar{\kappa}q\varepsilon(q)}\right]^2\left(1+\frac{q}{b}\right)^{-6}J_{N\pm 1N}(ql)J_{NN}(lq)$$
$$\pm 2\cdot 2\pi(\Delta d)^2\sum_q ql\left[\frac{\Gamma(q)}{\varepsilon(q)}\right]^2\exp\left(-\frac{1}{4}q^2d^2\right)J_{N\pm 1N}(lq)J_{NN}(lq). \tag{3.8}$$

3.4 Cyclotron resonance linewidth

As has been shown in ref. 17, the lineshape of the dynamical conductivity $\sigma_{xx}(\omega)$ depends strongly on the position of E_F at low temperatures. This is a result of the singular density of states characteristic of the two-dimensional system and causes the quantum oscillation of the cyclotron resonance (CR) lineshape. Therefore it is rather impossible to give an exact expression for the CR width. As a measure of the width we consider here the second moment of the spectrum. The actual linewidth is roughly the same as the moment in case of short-ranged scatterers. In case of slowly-varying scatterers, however, it can be much smaller than the moment.[17] The moment for the transition from the N-th to $N+1$-th level becomes

$$(\Gamma_{N\to N+1}^{CR})^2\equiv\frac{1}{2}(\Gamma_N^2+\Gamma_{N+1}^2-8\gamma_{NN+1NN+1}), \tag{3.9}^{17)}$$

where $\gamma_{NN+1NN+1}$ is the proper vertex part given in ref. 17. In the present model we have

$$(\Gamma_{N\to N+1}^{CR})^2=2N_i\sum_q\frac{1}{2q}\left[\frac{2\pi e^2}{\bar{\kappa}q\varepsilon(q)}\right]^2\left(1+\frac{q}{b}\right)^{-6}[J_{NN}(lq)-J_{N+1N+1}(lq)]^2$$
$$+2\cdot 2\pi(\Delta d)^2\sum_q\left[\frac{\Gamma(q)}{\varepsilon(q)}\right]^2\exp\left(-\frac{1}{4}q^2d^2\right)[J_{NN}(lq)-J_{N+1N+1}(lq)]^2. \tag{3.10}$$

A similar expression is obtained for the transition $N-1\to N$. The above result is calculated in the case that the N-th Landau level is completely filled or empty. Actually we have to take into account the partial occupation of levels, and the actual moment is expected to be a certain average of $\Gamma^{CR}_{N-1\to N}$ and $\Gamma^{CR}_{N\to N+1}$.

§4. Results and Discussion

In performing numerical calculation we shall use the following values of the parameters: $m_t=0.1905\,m_0$, $m_l=0.916\,m_0$, $\kappa_s=11.8$, $\kappa_{ox}=3.8$, and $N_{\rm depl}=1\times10^{11}\ {\rm cm}^{-2}$, where m_0 is the free electron mass. We shall use $g=2$ and neglect the enhancement of the g factor or the spin splitting caused by electron-electron interactions.[20] Further we completely neglect the valley splitting and its enhancement.[25] Assumed scatterers in the calculation are characterized by $N_i=3\times10^{17}\ {\rm cm}^{-3}$, $\Delta=3$ A, and $d=25$ A, which give the peak mobility of about $2.1\times10^4\ {\rm cm}^2/{\rm Vs}$ at $N_s\sim1.4\times10^{12}\ {\rm cm}^{-2}$. For convenience we define the width Γ, given by

$$\Gamma^2=\frac{2}{\pi}\hbar\omega_c\frac{\hbar}{\tau}, \tag{4.1}$$

where $\tau=\mu m/e$ is the relaxation time in the absence of a magnetic field. As has been shown in ref. 9, the above relation holds, if scatterers are of short range and the same for both $H=0$ and $H\neq0$.

The results for $H=150$ kOe are shown in Figs. 2 and 3. The level width Γ_N of the Landau level where E_F lies and the CR moments $\Gamma^{CR}_{N\to N+1}$ and $\Gamma^{CR}_{N-1\to N}$ are given in Fig. 2 together with the mobility for $H=0$ and Γ defined by eq. (4.1). The width Γ_N depends on the position of E_F and becomes very large when E_F lies at the tail region of each Landau level. The CR moments, however, do not vary so much with N_s. This means that the scattering potentials become long range because of the decrease of the screening effect when E_F lies at the tails. Except these cases, however, both Γ_N and the CR moments are well given by Γ. The additional structures appearing in Γ_N are due to the spin splitting. In Fig. 3 the peak values of the transverse conductivity σ_{xx} and $\Delta\sigma_{xy}$ are shown together with the results for short-ranged scatterers given by eq. (4.1). They become very small when E_F lies at the tail region, since the potentials become of slowly-varying type. When E_F lies near the center of the level, however, they are again well given by those for short-ranged scatterers.

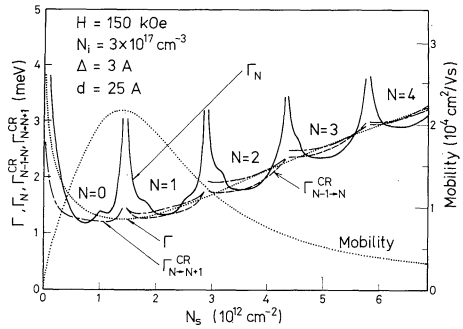

Fig. 2. Calculated widths as a function of N_s for $N_{\rm depl}=1\times10^{11}\ {\rm cm}^{-2}$ and $H=150$ kOe. The mobility at $H=0$ and the corresponding Γ are shown by the dotted lines.

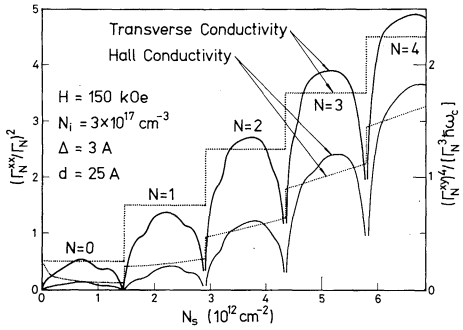

Fig. 3. Calculated peak values of σ_{xx} and $\Delta\sigma_{xy}$ in a unit of $e^2/\pi^2\hbar$ as a function of N_s for $H=150$ kOe and $N_{\rm depl}=1\times10^{11}\ {\rm cm}^{-2}$. The corresponding results for short-ranged scatterers are shown by the dotted lines for the sake of comparison.

Similar results for weaker magnetic fields are given in Figs. 4~7. With decreasing H the screening effect becomes rather small and consequently the peak value of σ_{xx} and $\Delta\sigma_{xy}$ decreases especially at low N_s where the charged impurities are dominant scatterers. This feature agrees with the experiments by Lakhani and Stiles,[13] who showed by a systematic measurement of the H dependence of σ_{xx} that its peak values decreased with the decrease of H more rapidly than the theoretical prediction[10] for perfectly short-ranged scatterers. Quantitatively speaking, however, the calculated H dependence is larger than the experiments. A possible reason might be that we have assumed too much charged impurities which

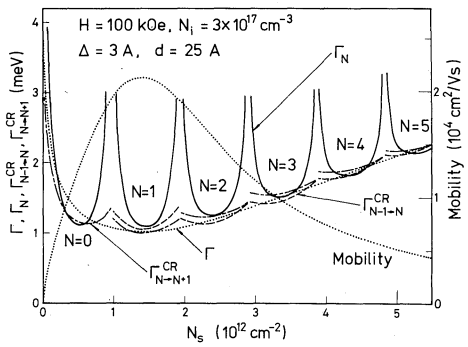

Fig. 4. Calculated widths as a function of N_s for $H=100$ kOe and $N_{\text{depl}}=1\times10^{11}$ cm^{-2}. The mobility at $H=0$ and the corresponding Γ are shown by the dotted lines.

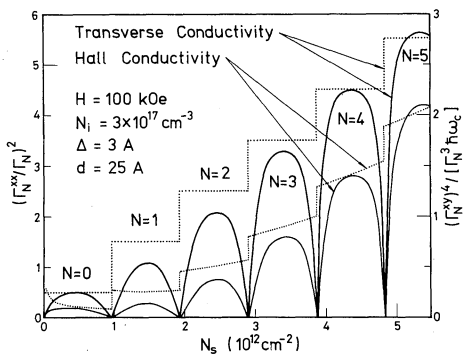

Fig. 5. Calculated peak values of σ_{xx} and $\Delta\sigma_{xy}$ in a unit of $e^2/\pi^2\hbar$ as a function of N_s for $H=100$ kOe and $N_{\text{depl}}=1\times10^{11}$ cm^{-2}. The corresponding results for short-ranged scatterers are shown by the dotted lines for the sake of comparison.

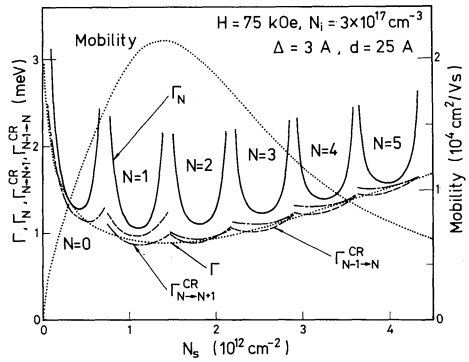

Fig. 6. Calculated widths as a function of N_s for $H=75$ kOe and $N_{\text{depl}}=1\times10^{11}$ cm^{-2}. The mobility at $H=0$ and the corresponding Γ are shown by the dotted lines.

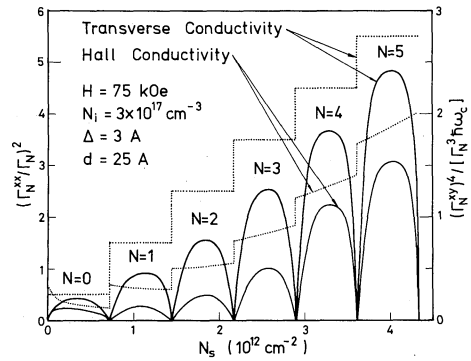

Fig. 7. Calculated peak values of σ_{xx} and $\Delta\sigma_{xy}$ in a unit of $e^2/\pi^2\hbar$ as a function of N_s for $H=75$ kOe and $N_{\text{depl}}=1\times10^{11}$ cm^{-2}. The corresponding results for short-ranged scatterers are shown by the dotted lines for the sake of comparison.

are long-ranged scatterers. As a matter of fact, the calculated N_s for the peak mobility is larger than the experimental N_s of usual samples. If we assume N_i which gives a proper N_s for the mobility peak, however, the peak mobility itself becomes much larger than those of usual samples. Matsumoto and Uemura introduced an additional scattering mechanism to explain the experimental N_s dependence of the mobility.[3] They assumed that the additional scatterers are rather of short-range. The present slight disagreement in strong H again suggests the existence of such a new scattering mechanism at N_s near the mobility peak.

In contrast to Γ_N the CR moments defined by eq. (3.9) are always almost the same as Γ. The CR width measured actually can be smaller than those and consequently than Γ at low N_s, where finite range of scatterers becomes important. This feature agrees with CR experiments by Abstreiter *et al.*[18] They have shown that the measured CR width is well given by eq. (4.1) at high N_s, where the surface roughness is considered to be dominant scatterers, and that it becomes smaller than eq. (4.1) at N_s near the mobility peak. With decreasing N_s it increses drastically, but this is attributed to inhomogeneous-type broadening. To make a quantitative comparison between the theory and the experiments, one must calculate the magnetic field dependence of $\sigma_{xx}(\omega)$ for finite-ranged scatterers. This is, however, not feasible under actual experimental conditions where a coupling between different Landau levels is rather important.

One important conclusion deduced from the above results is that one can use eq. (4.1)

in the estimation of the level width in strong H except when E_F lies at the tail region. This might be surprising if we consider the marked change of the density of states and consequently that of the screening effect in strong H. We have performed numerical calculation for various values of N_i, Δ, and d. The results depend rather only on the product Δd instead of each value of Δ and d, if d is not too large ($d \lesssim 30$ A). Further the above conclusion is shown to hold for large range of N_i and Δd which gives reasonable N_s dependence of the mobility. Thus one can conclude that Γ is the good measure of the actual widths in strong H for usual inversion layers.

In performing a lineshape analysis of the conductivity especially in strong H one has to take into account the finite range of scattering potentials and the screening effect in addition to the enhancement of the spin and valley splitting caused by electron-electron interactions. Such work has not been done yet and is left for future study. The existence of the strong and long-ranged potential can cause a strong localization of electrons when E_F lies close to the spectral edges. This might explain recent experiments of Kawaji and Wakabayashi,[16] who showed that there exists a region of N_s near the spectral edges, where σ_{xx} vanishes. Two mechanisms were proposed so far to explain the experiments. Aoki and Kamimura proposed the Anderson localization of electrons caused by potential fluctuation.[26] The Wigner crystallization was proposed by Kawaji and Wakabayashi,[16,27] and theoretically studied by Fukuyama[28] and by Tsukada.[29] In any case the large and long range potential fluctuations are considered to play important roles in these phenomena.

Acknowledgements

This work was started while the author stayed at Physik-Department, Technische Universität München, 8046 Garching bei Müchen, Fed. Rep. Germany as a research fellow of the Allexander von Humboldt Foundation. He is indebted to Professor Y. Uemura for reading the manuscript. The numerical computation was performed with the aid of HITAC 8800/8700 of the Computer Centre at the University of Tokyo. This work was partially supported by the Grant-in-Aid for Fundamental Scientific Research from the Ministry of Education.

Appendix Field Disturbance Associated with Surface Roughness

The surface roughness causes a change of the electron density distribution in the z direction, $n(z-\Delta(\boldsymbol{r}))-n(z)=-\Delta(\boldsymbol{r})\partial n/\partial z$. This gives the potential energy at $(\boldsymbol{r}, z)$

$$-\sum_{\boldsymbol{q}}\frac{2\pi e^2}{\kappa_s q}\Delta(\boldsymbol{q})N_s\,e^{i\boldsymbol{q}\cdot\boldsymbol{r}}\int dz'\,e^{-q|z-z'|}\frac{\partial n(z')}{\partial z'}$$
$$-\sum_{\boldsymbol{q}}\frac{2\pi e^2(\kappa_s-\kappa_{ox})}{\kappa_s(\kappa_s+\kappa_{ox})q}N_s\Delta(\boldsymbol{q})\,e^{i\boldsymbol{q}\cdot\boldsymbol{r}}\int dz'\,e^{-q(z+z')}\frac{\partial n(z')}{\partial z'}, \qquad (A\cdot 1)$$

to the lowest order with respect to $\Delta(\boldsymbol{r})$. In addition to the above we have to include a change of the electric field distribution induced by deformed Si–SiO_2 interface. It is given by

$$\sum_{\boldsymbol{q}}\frac{4\pi e^2(\kappa_s-\kappa_{ox})}{\kappa_s(\kappa_s+\kappa_{ox})}(N_{\mathrm{depl}}+N_s)\Delta(\boldsymbol{q})\,e^{i\boldsymbol{q}\cdot\boldsymbol{r}}\,e^{-qz}, \qquad (A\cdot 2)$$

to the first order in $\Delta(\boldsymbol{r})$. The roughness also causes the modification of the image potential. This was calculated by Saitoh[30] and is given by

$$\sum_{\boldsymbol{q}}\frac{(\kappa_s-\kappa_{ox})e^2}{4\kappa_s(\kappa_s+\kappa_{ox})}q^2\Delta(\boldsymbol{q})\,e^{i\boldsymbol{q}\cdot\boldsymbol{r}}\left[\frac{K_1(qz)}{qz}-\frac{1}{2}\frac{\kappa_s-\kappa_{ox}}{\kappa_s+\kappa_{ox}}K_0(qz)\right]. \qquad (A\cdot 3)$$

After a little rearrangement one gets eq. (2.24).

References

1) See, for example, F. Stern: CRC Critical Reviews in Solid State Sciences **4** (1974) 499 and references therein.
2) F. Stern and W. E. Howard: Phys. Rev. **163** (1967) 816.
3) Y. Matsumoto and Y. Uemura: *Proc. Int. Conf.*

Solid Surfaces, Kyoto, 1974, Japan. J. appl. Phys. (1974) Suppl. 2, Pt. 2, p. 367.
4) A. Hartstein, T. H. Ning and A. B. Fowler: *Proc. Int. Conf. Electronic Properties of Quasi-Two-Dimensional Systems, Providence, 1976*. Surface Sci. **58** (1976) 178.
5) R. E. Prange and T. Nee: Phys. Rev. **168** (1968) 779.
6) A. B. Fowler, F. F. Fang, W. E. Howard and P. J. Stiles: *Proc. Int. Conf. Phys. Semiconductors, Kyoto, 1966*, J. Phys. Soc. Japan **21** (1966) Suppl. p. 331.
7) T. Ando, Y. Matsumoto, Y. Uemura, M. Kobayashi and K. F. Komatsubara: J. Phys. Soc. Japan **32** (1972) 859.
8) K. F. Komatsubara, K. Narita, Y. Katayama, N. Kotera and M. Kobayashi: J. Phys. Chem. Solids **35** (1974) 723.
9) T. Ando and Y. Uemura: J. Phys. Soc. Japan **36** (1974) 959.
10) T. Ando: J. Phys. Soc. Japan **36** (1974) 1521; **37** (1974) 622; **37** (1974) 1044.
11) T. Ando, Y. Matsumoto and Y. Uemura: J. Phys. Soc. Japan **39** (1975) 279.
12) S. Kawaji, T. Igarashi and J. Wakabayashi: Progr. theor. Phys. Suppl. **57** (1975) 176.
13) A. A. Lakhani and P. J. Stiles: Phys. Rev. **B13** (1976) 5386.
14) R. R. Gerhardts: Z. Phys. **B21** (1975) 275; **B21** (1975) 285.
15) T. Ando: Z. Phys. **B24** (1976) 219.
16) S. Kawaji and J. Wakabayashi: *Proc. Int. Conf. Electronic Properties of Quasi-Two-Dimensional Systems, Providence, 1976*, Surface Sci. **58** (1976) 238.
17) T. Ando: J. Phys. Soc. Japan **38** (1975) 989.
18) G. Abstreiter, J. P. Kotthaus, J. F. Koch and G. Dorda: Phys. Rev. **B14** (1976) 2480.
19) T. Ando: Phys. Rev. Letters **36** (1976) 1383.
20) T. Ando and Y. Uemura: J. Phys. Soc. Japan **37** (1974) 1044.
21) F. Stern: Phys. Rev. Letters **18** (1967) 546.
22) Y. Matsumoto: Private communication.
23) D. C. Tsui and G. Kaminsky: Phys. Rev. Letters **35** (1975) 1468.
24) W. E. Howard and F. F. Fang: Phys. Rev. **B13** (1976) 2519.
25) F. J. Ohkawa and Y. Uemura: J. Phys. Soc. Japan **43** (1977) 907.
26) H. Aoki and H. Kamimura: Solid State Commun. **21** (1977) 45.
27) S. Kawaji and J. Wakabayashi: Solid State Commun. **22** (1977) 87.
28) H. Fukuyama: Solid State Commun. **19** (1976) 551.
29) M. Tsukada: J. Phys. Soc. Japan **42** (1977) 391.
30) M. Saitoh: J. Phys. Soc. Japan **42** (1977) 201.